

Original Research

HnRNP A1 Suppresses the Odontogenic Differentiation and the Inclusion of RUNX2 Exon 5 of Dental Mesenchymal Cells

Yanan Zhang¹, Junjun Huang¹, Lingyan Yan¹, Rong Jia¹, Jihua Guo^{1,2,*}

¹The State Key Laboratory of Oral & Maxillofacial Reconstruction and Regeneration, Key Laboratory of Oral Biomedicine Ministry of Education, Hubei Key Laboratory of Stomatology, School & Hospital of Stomatology, Wuhan University, 430079 Wuhan, Hubei, China

²Department of Endodontics, School & Hospital of Stomatology, Wuhan University, 430079 Wuhan, Hubei, China

*Correspondence: [jihua guo@whu.edu.cn](mailto:jihuaguo@whu.edu.cn) (Jihua Guo)

Academic Editors: Ana Caruntu and Cristian Scheau

Submitted: 10 December 2022 Revised: 2 March 2023 Accepted: 8 March 2023 Published: 19 July 2023

Abstract

Background: RUNX2 (Runt-related transcription factor 2) acts as a key regulator in the odontogenic differentiation of human dental pulp stem cells (hDPSCs). Moreover, the inclusion of exon 5 is important for RUNX2 function. Our previous study showed that Y-Box Binding Protein 1 (YBX1) promoted RUNX2 exon 5 inclusion and mineralization of hDPSCs. However, the regulatory mechanism of RUNX2 exon 5 alternative splicing needed further exploration. **Methods:** The expression level of heterogeneous nuclear ribonucleoprotein A1 (hnRNP A1) during the odontogenic differentiation of hDPSCs was analyzed by RT-PCR and Western blot. The roles of hnRNP A1 in the alternative splicing of RUNX2 exon 5 and the odontogenic differentiation of dental mesenchymal cells were analyzed by gain- and loss-of-function experiments. **Results:** Surprisingly, we found an alternative splicing factor, hnRNP A1, which had an opposite role to YBX1 in regulating RUNX2 exon 5 inclusion and odontogenic differentiation of hDPSCs. Through gain- and loss-of-function assay, we found that hnRNP A1 suppressed the inclusion of RUNX2 exon 5, resulting in the inhibition of odontoblastic differentiation. The overexpression of hnRNP A1 can inhibit the expression of ALP (alkaline phosphatase) and OCN (osteocalcin), and the formation of mineralized nodules during the odontogenic differentiation of both hDPSCs and mouse dental papilla cells (mDPCs), whereas the opposite results were obtained with an hnRNP A1 knockdown preparation. **Conclusions:** The present study indicated that hnRNP A1 suppressed RUNX2 exon 5 inclusion and reduced the odontogenic differentiation ability of hDPSCs and mDPCs.

Keywords: dental pulp stem cells; hnRNP A1; odontogenic differentiation; RUNX2

1. Introduction

RUNX2 (Runt-related transcription factor 2), a transcription factor containing the Runt structural domain, is a master regulator in osteogenesis and tooth development [1,2]. During the development of the mouse tooth, Runx2 is highly expressed in the dental papilla and follicle mesenchyme at embryonic day 14 [3]. In addition, Runx2 mediates the epithelial-mesenchymal interactions during the bud-to-cap-stage transition of tooth development [4]. These results suggested that Runx2 is essential for tooth development. RUNX2 encodes a highly conserved transcription factor, containing an essential Runt domain, which is involved in DNA binding [5], heterodimerization [6], and nuclear location [7]. RUNX2 exon 5 encodes a nuclear localization signal (NLS) and partial C-terminus of the Runt domain [8]. Two shorter isoforms of RUNX2 without exon 5 (RUNX2 Δ 5 and RUNX2 Δ 5 Δ 7) can not localize to the nucleus and bind DNA, indicating that the exclusion of exon 5 impaired the function of RUNX2 [9]. Our previous study found that RUNX2 exon 5 inclusion increases during the process of mineralization of human dental pulp stem cells (hDPSCs), and is crucial for the differentiation of those cells [10]. Moreover, splicing factor Y-box binding protein 1 (YBX1) promotes RUNX2 exon 5 inclusion and plays a

positive role in the differentiation of hDPSCs [10]. However, the regulatory mechanism of RUNX2 exon 5 alternative splicing needs to be further explored.

Splicing factor heterogeneous nuclear ribonucleoprotein A1 (hnRNP A1) is one of the most plentiful and extensively expressed nuclear proteins [11]. The hnRNP A1 protein encompasses an N-terminal region with two closely-related RRM domains (RRM1 and RRM2), and a glycine-rich C-terminal region with an RGG box domain relating to RNA binding, and an M9 domain relating to nuclear targeting [12,13]. HnRNP A1 is a multifunctional protein that participates in mRNA biogenesis, such as transcription, alternative splicing, and stability [13,14]. As a classical modulator of alternative splicing, hnRNP A1 has been extensively studied [13]. Recently, several studies have elucidated the biological roles of hnRNP A1 in the differentiation of some stem cells [15,16], but the functions of hnRNP A1 in differentiation of hDPSCs remain unknown.

The hDPSCs are characterized by a rapid proliferation rate, self-renewal capability, and high accessibility to multi-directional differentiation (e.g., odontogenic, osteogenic, chondrogenic, and neurogenic) [17,18]. Many studies have demonstrated that hDPSCs possesses the potential to form dentin/pulp-like structure, as well as to compensate for de-



fects in dentin and bone formation [19,20]. But the regulatory mechanisms of hDPSC differentiation are not fully understood.

In the present study, we attempted to analyze the function of hnRNP A1 in RUNX2 exon 5 alternative splicing and odontogenic differentiation of hDPSCs and mouse dental papilla cells (mDPCs).

2. Materials and Methods

The collection of human dental pulp tissues was approved by the Ethics Committee of the School and Hospital of Stomatology at Wuhan University (2019-A47). Informed consent was obtained from every participant. The use of animal tissues was approved by the Animal Welfare and Ethics Committee of the School and Hospital of Stomatology at Wuhan University (S07922090F).

2.1 Cells Isolation, Culture and Identification

Human dental pulp tissues were isolated from healthy and non-functional third molars donated by patients aged 18–26 years old. In brief, healthy dental pulp tissues were collected and cut into tiny pieces in a sterile environment, and then digested with 3 mg/mL collagenase type I (#SCR103, Sigma-Aldrich, Saint Louis, MO, USA) for 1 h at 37 °C. The cells were cultured in minimal essential medium, alpha modification (#SH30625.01, Hyclone, Marlborough, MA, USA), which contains 10% fetal bovine serum (#10099141, Gibco, Carlsbad, CA, USA), 100 U/mL penicillin, and 100 mg/mL streptomycin (#15240-062, Gibco, Carlsbad, CA, USA). The surface stemness markers of hDPSCs were determined by flow cytometry. In brief, hDPSCs (3rd passage) were digested with trypsin and rinsed two times with phosphate-buffered saline (PBS) (#SH30256.01, Hyclone, Marlborough, MA, USA). Then, cells were resuspended with flow cytometry staining buffer (#S1001, MultiSciences, Hangzhou, China), followed by incubation with the following fluorescent dye-conjugated antibodies for 30 minutes: isotype control-anti-CD34 (#400207); anti-CD34 (#343603); isotype control-anti-CD45 (#400109); anti-CD45 (#368507); isotype control-anti-CD29, CD90, and CD146 (#400111); anti-CD29 (#303003); anti-CD90 (#328109); and anti-CD146 (#361005) (all antibodies were obtained from Biotend, San Diego, CA, USA). The stained cells were analyzed by a CytoFLEX Flow Cytometer (#C09748, Beckman, Indianapolis, IN, USA). CD34 and CD45 are hematopoietic stem cells and leukocyte markers, whereas CD29, CD90, and CD146, are mesenchymal stem cell (MSC) markers. Analysis of data was performed with CytExpert software (Beckman, Indianapolis, IN, USA).

Mice were raised in a specific pathogen-free facility with a 12:12-h day/night cycle. Primary mDPCs were isolated from the first mandibular molars of C57BL/6 mice at postnatal day 0.5 (PN 0.5) and digested by 0.25% trypsin (#SH30042.02, Hyclone, Marlborough, MA, USA) for 10

min, and primary cells were fusiform or triangular under phase contrast microscope (**Supplementary Fig. 1**). CAL 27 cells, HEK 293 cells and HEK 293T cells were authenticated using short tandem repeat (STR) profiling analysis. Mycoplasma testing has been done for the cell lines used. The mDPCs, CAL 27 cells, HEK 293 cells, and HEK 293T cells, were grown in Dulbecco's modified Eagle medium (DMEM) (#SH30022.01, Hyclone, Marlborough, MA, USA), which contains 10% fetal bovine serum.

To induce differentiation, hDPSCs and mDPCs were cultured in differentiation medium which comprised basal medium, 10 nM dexamethasone (#T5648, Sigma-Aldrich, Saint Louis, MO, USA), 50 µg/mL ascorbic acid (#A4544, Sigma-Aldrich, Saint Louis, MO, USA) and 10 mM β-glycerophosphate (#G9422, Sigma-Aldrich, Saint Louis, MO, USA). All cells were incubated at 37 °C in 5% CO₂ humidified air.

2.2 Plasmids and Transfection

T7-tagged human hnRNP A1 overexpression plasmid was made for our previous publication [21]. The mouse hnRNP A1 gene was amplified using primers 5'-ATGTCTAAGTCCGAGTCTCCCA-3' and 5'-GAACCTCCTGCCACTGCCATA-3'. Then, the product was amplified with 5'-TTCCGAAGCTTGCCACCATGTCTAAGTCCGAGTCTCCCA-3' and 5'-TTCCGGAATTCCCGAACCTCCTGCCACTGCCATA-3', and cloned into the p3xFlag-CMV-14 at HindIII and EcoRI sites. The FLAG-fusion fragment was amplified with 5'-TTCCGACTAGTGCCACCATGTCTAAGTCCGAGTCTCCCA-3' and 5'-TTCGCGGATCCCTACTTGTTCATCGT-CATCCTTG-3', and cloned into the pLVX-IRES-Puro at SpeI and BamHI sites to obtain recombinant expression plasmids 3xFLAG-tagged hnRNP A1.

A minigene of human RUNX2 with genomic DNA sequence from exon 4 to exon 6 (including exon 4, exon 5, exon 6, and partial intron) was amplified from the CAL 27 genome by the following primers: 5'-CACCTTGACCATAACCGTCTTAC-3' and 5'-TACTAGAGCATGACCAAACAACAGTG-3', used to amplified exon 4 and intron 4 (535 bp downstream of exon 4); 5'-AAAGAAAAGTCACTATGGTCATCGTG-3' and 5'-AGCCACACATTGACCTTGCCT-3', used to amplified intron 4 (494 bp upstream of exon 5), exon 5 and intron 5 (481 bp downstream of exon 5); 5'-CCCTCCATTCTCATTCTGC-3' and 5'-ATCGGTGATGGCAGGAAGC-3', used to amplified intron 5 (617 bp upstream of exon 6). Then, the three fragments were cloned into the pEGFP-N1 vector using In-Fusion Cloning at EcoRI and BamHI sites. HEK 293 cells were transfected with plasmids using Lipofectamine 2000 (#11668019, Invitrogen, Carlsbad, CA, USA). HEK 293T cells were cotransfected with lentiviral backbone plasmids (T7-tagged hnRNP A1, 3xFlag-tagged hnRNP

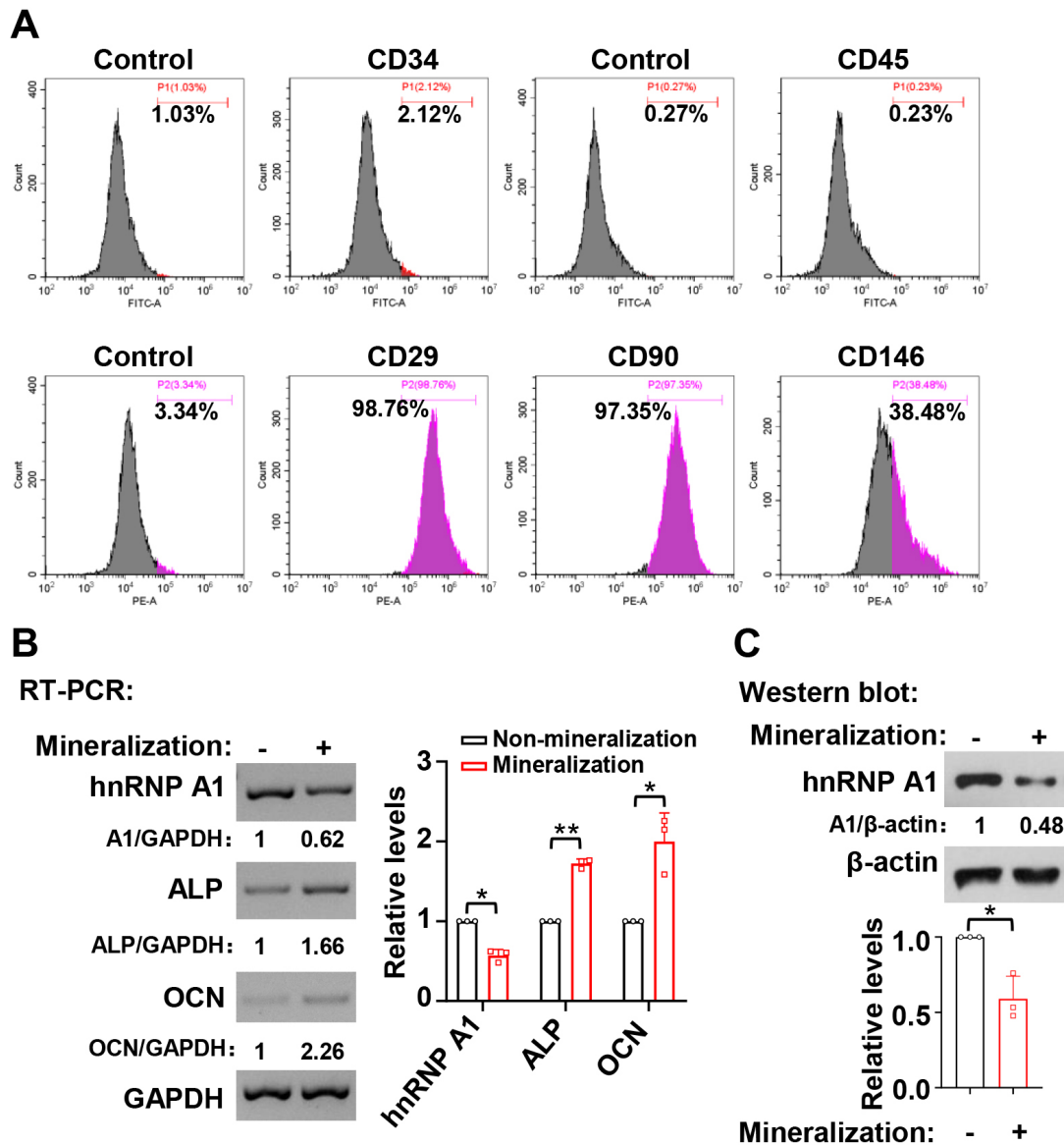


Fig. 1. HnRNP A1 expression decreased during the mineralization induction in hDPSCs. (A) The expression of cell surface markers on hDPSCs was analyzed by flow cytometric. (B) RNA expression levels of ALP and OCN increased while the levels of hnRNP A1 decreased after seven days of mineralization induction. Histogram showed quantification for the relative RNA expression levels of hnRNP A1, ALP, and OCN, $n = 3$. GAPDH served as a loading control. (C) The corresponding protein expression levels of hnRNP A1 decreased after seven days of mineralization in hDPSCs. Histogram showed quantification for the relative protein expression levels of hnRNP A1, $n = 3$. β -actin served as a loading control. *: $p < 0.05$; **: $p < 0.01$. ALP, alkaline phosphatase; OCN, osteocalcin.

A1, or control vector pLVX-IRES-puro), packaging plasmid psPAX2, and envelope plasmids pMD2.G. The supernatants containing lentiviral particles were collected 48 h after transfection and clarified by a 0.45 μm filter. The hDPSCs or mDPCs were then transfected with supernatants.

2.3 RNA Interference (RNAi) and Transfection

The sequences of hnRNP A1 siRNAs are as follows: 5'-GUGGUAUGAGAGAUCCAATT-3' (siA1-1) and 5'-GCUCUUAUUGGAGGGUUGTT-3' (siA1-2) for human, and 5'-GUAUCCAUAUCAUGUGUATT-3' (siA1-

3) for mouse. Nonspecific siRNA (NS) was obtained from Sangon Biotech (Shanghai, China). Cells were transfected with 20 nM siRNA by using Lipofectamine 3000 (#L3000015, Invitrogen, Carlsbad, CA, USA) according to the manufacturer's instructions. After 48 h, cells were transfected again.

2.4 Western Blot

Total cellular protein samples were lysed with 2 \times SDS sample buffer, then denatured at 95 $^{\circ}\text{C}$ for 3 min. Protein samples were loaded onto 4–12% SDS-PAGE gel (#M00929, GenScript, Nanjing, China) and transferred to

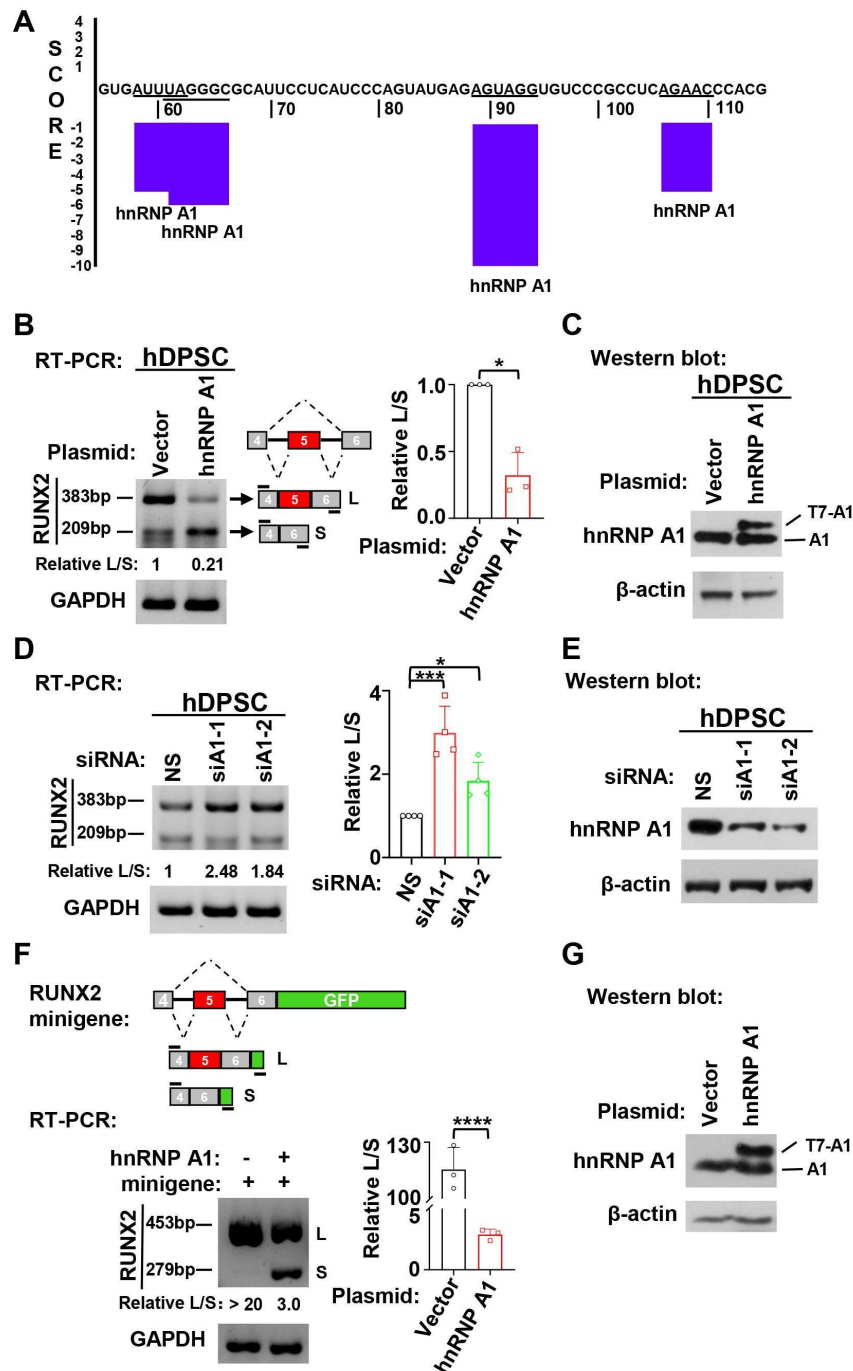


Fig. 2. HnRNP A1 suppressed the inclusion of RUNX2 exon 5. (A) HnRNP A1 binding sites in human RUNX2 exon 5 RNA sequence were predicted by SpliceAid online program. Negative score represents suppressing exon inclusion. (B) Overexpression of hnRNP A1 suppressed RUNX2 exon 5 inclusion in hDPSCs. The ratio of inclusion versus exclusion of RUNX2 exon 5 in hDPSCs was represented by histogram, $n = 3$. GAPDH served as a loading control. (C) Overexpression of exogenous T7-tagged hnRNP A1 in hDPSCs was confirmed by Western blot. β -actin served as a loading control. (D) Knockdown of hnRNP A1 promoted RUNX2 exon 5 inclusion in hDPSCs. The ratio of inclusion versus exclusion of RUNX2 exon 5 in hDPSCs was represented by histogram, $n = 4$. GAPDH served as a loading control. (E) Knockdown efficiency of hnRNP A1 was analyzed by Western blot. (F) Overexpression of hnRNP A1 suppressed the inclusion of RUNX2 exon 5 in a minigene in HEK 293 cells. RT-PCR was performed to analyze the alternative splicing of exon 5 of RUNX2 minigene with or without hnRNP A1 overexpression. Schematic diagram of RUNX2 exon 5 minigene was presented. The histogram showed the statistical analysis of the ratios of the inclusion versus exclusion of RUNX2 exon 5 in minigene, $n = 3$. GAPDH served as a loading control. (G) Overexpression of exogenous T7-tagged hnRNP A1 in HEK 293 cells was confirmed by Western blot. β -actin served as a loading control. *: $p < 0.05$; ***: $p < 0.001$; ****: $p < 0.0001$.

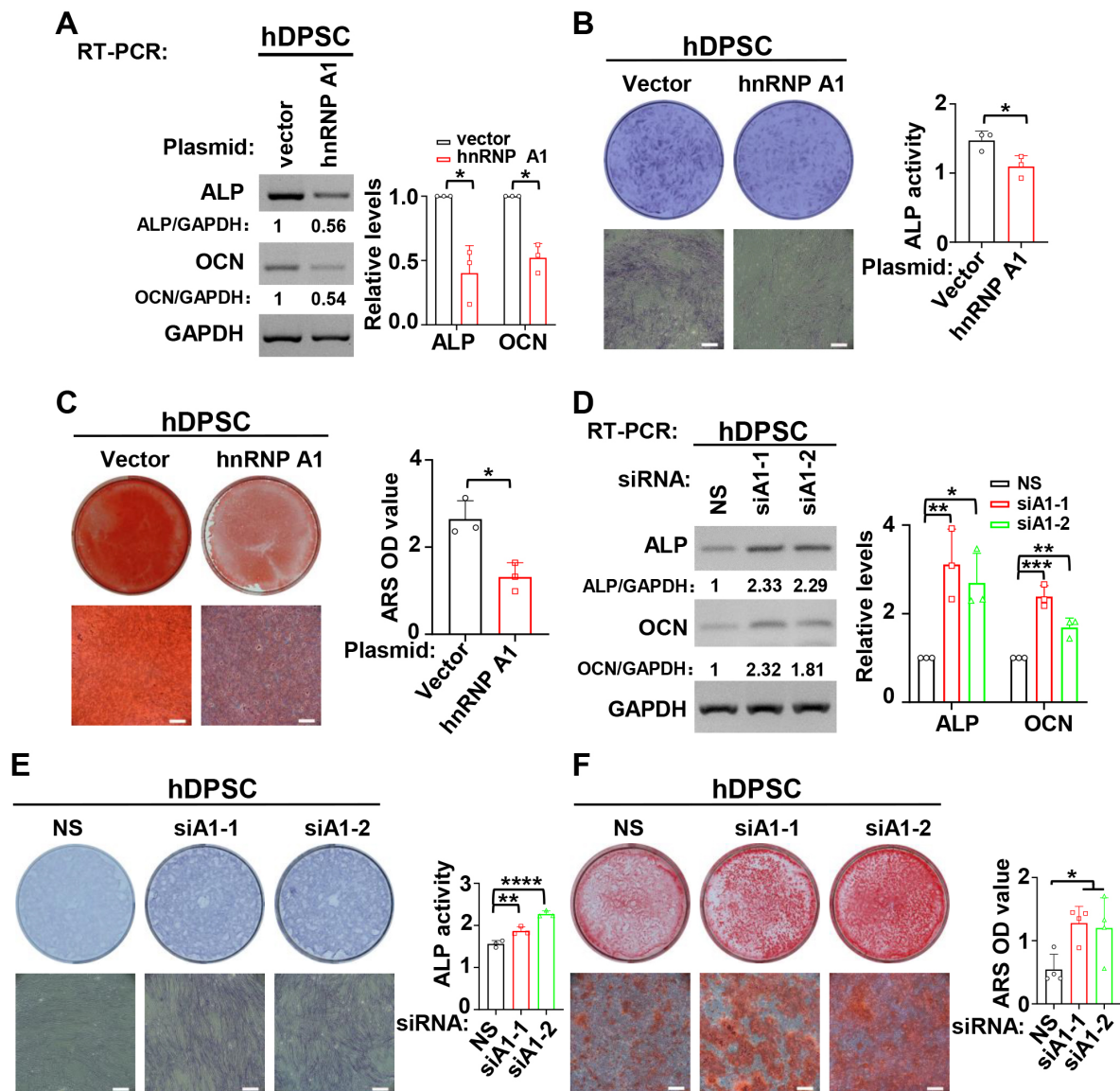


Fig. 3. HnRNP A1 inhibited the differentiation of hDPSCs. (A–C) During the process of mineralization induction, overexpression of hnRNP A1 decreased the expression of ALP and OCN (A), ALP activity (B), and the formation of mineralized nodules (C). Alizarin red staining (ARS) was applied to stain mineralized nodules after hDPSCs were cultured in differentiation medium for 14 days. Mineralized nodules were collected with 10% cetylpyridinium chloride and the absorbance values at 562 nm were measured for quantification of mineralized nodules. Histogram respectively showed quantification for the expression of ALP and OCN, ALP activity or the formation of mineralized nodules, $n = 3$. GAPDH served as a loading control. Scale bar = 500 μm . (D–E) HnRNP A1 knockdown increased the expression of ALP and OCN (D), ALP activity (E) and the formation of mineralized nodules (F). ARS was applied to stain mineralized nodules after hDPSCs cultured in differentiation medium for 14 days. Histogram respectively showed quantification for the expression of ALP and OCN ($n = 3$), ALP activity ($n = 3$) or the formation of mineralized nodules ($n = 4$). GAPDH served as a loading control. Scale bar = 500 μm . *: $p < 0.05$; **: $p < 0.01$; ***: $p < 0.001$; ****: $p < 0.0001$.

nitrocellulose membranes. After blocking in 5% non-fat milk for 1 h, the membranes were incubated with the following antibodies: mouse monoclonal anti-hnRNP A1 (#sc-32301, Santa Cruz Biotechnology, Dallas, TX, USA); mouse monoclonal anti- β -actin (#66009-1-Ig, Proteintech, Wuhan, China); and rabbit polyclonal anti-FLAG (#20543-1-AP, Proteintech, Wuhan, China).

2.5 Reverse Transcription-Polymerase Chain Reaction (RT-PCR)

Total RNA was extracted using the AxyPrep miniprep kit (#AP-MN-MS-RNA-250, Axygen, Union City, CA, USA). RNA was reversely transcribed to cDNA by using Maxima H Minus Transcriptase (#EP0752, Thermo Fisher Scientific, Carlsbad, CA, USA), and amplified with Green Taq Mix (#P131, Vazyme, Nanjing, China) according

to the manufacturer's protocols. Sequences of primers were as follows: 5'-GACGAGGCAAGAGTTTCACC-3' and 5'-GGTGGTAGAGTGGATGGACG-3' for endogenous RUNX2 exon 5 alternative splicing; 5'-CACCTTGACCATAACCGTCTTCAC-3' and 5'-GCTCCTCGCCCTTGCTACCA-3' for exogenous RUNX2 exon 5 alternative splicing; 5'-AAGCAATTTTGGAGGTGGTG-3' and 5'-ATAGCCACCTTGGTTTCGTG-3' for hnRNP A1; 5'-GACAAGAAGCCCTTCACTGC-3' and 5'-AGACTGCGCCTGGTAGTTGT-3' for alkaline phosphatase (ALP); 5'-CTACCTGTATCAATGGCTGGGAG-3' and 5'-TGGTCAGCCAACTCGTCACAG-3' for osteocalcin (OCN); 5'-GAAGGTGAAGTCCGGAGTC-3' and 5'-GAAGATGGTGTGGGATTTTC-3' for GAPDH; 5'-GACGAGGCAAGAGTTTCACC-3' and 5'-CGTGGTGGAGTGGATGGATG-3' for mouse Runx2 exon 5 alternative splicing; 5'-CCAACTCTTTGTGCCAGAGA-3' and 5'-TGGCTACATTGGTGTGAGCT-3' for mouse Alp; 5'-CACCATGAGGACCCTCTCTC-3' and 5'-TGGACATGAAGGCTTTGTCA-3' for mouse Ocn; 5'-AAGGTCATCCCAGAGCTGAA-3' and 5'-CTGCTTACCACCTTCTTGA-3' for mouse Gapdh.

2.6 Alkaline Phosphatase Staining and Activity

After being cultured in differential medium for 7 days, the cells were rinsed three times with PBS and fixed with 4% paraformaldehyde for 15 min. Then, cells were washed with PBS for three times and alkaline phosphatase staining was performed with a BCIP/NBT ALP Color Development Kit (#C3206, Beyotime, Shanghai, China) according to the manufacturer's instructions. The ALP activity of the harvested proteins was measured with an ALP activity kit (#A059-2-2, Jiancheng, Nanjing, China), and the absorbance values at 520 nm were measured. ALP activity relative to that of the control group was calculated after normalization with the total protein level.

2.7 Alizarin Red Staining (ARS) and Quantification

After hDPSCs were cultured in differentiation medium for 14 days or mDPSCs were cultured in differentiation medium for 7 days, cells were rinsed three times with PBS and fixed with 4% paraformaldehyde for 15 min. Then, cells were washed with PBS for three times. Calcium deposition was stained with ARS (#ALIR10001, Cyagen, Suzhou, China). Furthermore, mineralized nodules were dissolved in 10% cetylpyridinium chloride (#C129534, aladdin, Shanghai, China). The concentration of calcium was calculated by measuring the absorbance value at 562 nm.

2.8 Statistical Analysis

All statistical analyses were performed using GraphPad Prism 8.0 (San Diego, CA, USA). Student's *t* tests

were used to analyze the statistical differences between two groups. One-way analysis of variance was performed for the comparison among three groups.

3. Results

3.1 HnRNP A1 Expression is Reduced During Mineralization Induction of hDPSCs

We explored the expression profile of hnRNP A1 during the mineralization induction of hDPSCs. Primary hDPSCs were isolated from extracted third molars, and the surface markers were analyzed. The results showed that these cells were positive for the MSC markers, including CD29, CD90, and CD146, although they were negative for the hematopoietic stem cells and leukocyte markers like CD34 and CD45 (Fig. 1A). In the current study, hnRNP A1 expression showed reduced at RNA (Fig. 1B) and protein (Fig. 1C) levels after hDPSC mineralization induction for 7 days. The expression levels of ALP and OCN were applied to represent the mineralized state of hDPSCs (Fig. 1B).

3.2 HnRNP A1 Suppresses RUNX2 Exon 5 Inclusion

Our previous study demonstrated that the inclusion of RUNX2 exon 5 is enhanced during the odontogenic differentiation of hDPSCs [10]. To explore whether hnRNP A1 participates in RUNX2 exon 5 alternative splicing, we applied an online RNA binding sequence database, SpliceAid. We found that RUNX2 exon 5 has four potential binding sites for hnRNP A1 (Fig. 2A). We further explored the role of hnRNP A1 in the alternative splicing of RUNX2 exon 5 by gain- and loss-of-function experiments. We found that overexpression of hnRNP A1 significantly suppressed RUNX2 exon 5 inclusion in hDPSCs (Fig. 2B,C). In contrast, in the hnRNP A1 knockdown, there was a markedly increased RUNX2 exon 5 inclusion (Fig. 2D,E). To confirm the inhibition of hnRNP A1 on the inclusion of RUNX2 exon 5, we co-transfected HEK 293 cells with RUNX2 exon 5 minigene and hnRNP A1 expression plasmid. Consistently, hnRNP A1 overexpression notably suppressed RUNX2 exon 5 inclusion compared with the control group in the minigene system (Fig. 2F). These results suggested that hnRNP A1 suppressed the inclusion of RUNX2 exon 5.

3.3 HnRNP A1 Inhibits the Odontogenic Differentiation of hDPSCs

Next, the function of hnRNP A1 in the odontogenic differentiation of hDPSCs was investigated. The expression levels of ALP and OCN were reduced after overexpression of hnRNP A1 in the mineralization induced hDPSCs (Fig. 3A). Meanwhile, ALP activity (Fig. 3B) and the formation of mineralized nodules were reduced in hDPSCs with overexpressed hnRNP A1 (Fig. 3C). Conversely, knockdown of hnRNP A1 led to a great increase in the expression of ALP and OCN in mineralized hDPSCs (Fig. 3D). ALP activity (Fig. 3E) and the formation of min-

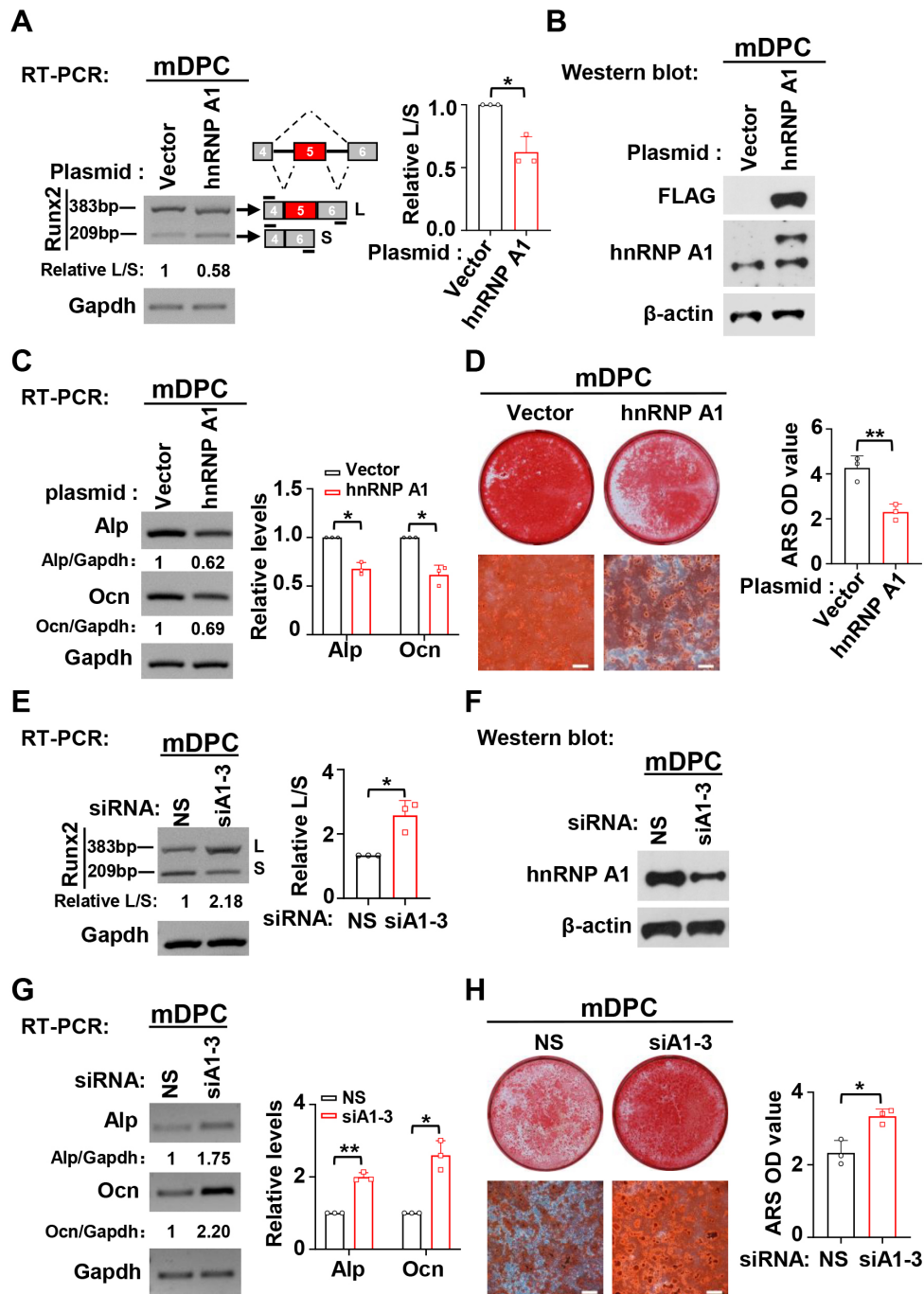


Fig. 4. HnRNP A1 suppresses the inclusion of Runx2 exon 5 and differentiation in mDPCs. (A) Overexpression of hnRNP A1 suppressed the inclusion of Runx2 exon 5. Bar graph showed the summarized ratio of inclusion versus exclusion of Runx2 exon 5, $n = 3$. Gapdh served as a loading control. (B) Overexpression of exogenous FLAG-tagged hnRNP A1 was confirmed by Western blot. Actin served as a loading control. (C,D) Overexpression of hnRNP A1 reduced the expression of Alp and Ocn (C) and the formation of mineralized nodules (D). ARS was applied to stain mineralized nodules after mDPCs cultured in differentiation medium for 7 days, Scale bar = 500 μm . Histogram showed quantification for the expression of Alp and Ocn, or the formation of mineralized nodules, $n = 3$. Gapdh served as a loading control. (E) Knockdown of hnRNP A1 promoted the inclusion of Runx2 exon 5. Bar graph showed the summarized ratio of inclusion versus exclusion of Runx2 exon 5, $n = 3$. Gapdh served as a loading control. (F) Knockdown efficiency of hnRNP A1 was analyzed by Western blot. β -actin served as a loading control. (G,H) Knockdown of hnRNP A1 increased the expression of Alp and Ocn (G) and the formation of mineralized nodules (H). ARS was applied to stain mineralized nodules after mDPCs cultured in differentiation medium for 7 days, Scale bar = 500 μm . Histogram showed quantification for the expression of Alp and Ocn, or the formation of mineralized nodules, $n = 3$. Gapdh served as a loading control. *: $p < 0.05$; **: $p < 0.01$.

eralized nodules (Fig. 3F) were also promoted in hDPSCs with hnRNP A1 knockdown. These results demonstrated that hnRNP A1 inhibited the mineralization of hDPSCs.

3.4 HnRNP A1 Suppresses the Inclusion of Mouse Runx2 Exon 5 and Odontogenic Differentiation of mDPCs

According to our previous study, RUNX2 exon 5 is highly conserved in human and mouse except for one nucleotide replacement [10]. Therefore, we speculated that hnRNP A1 may also suppress mouse Runx2 exon 5 inclusion and odontogenic differentiation in mDPCs. As we speculated, hnRNP A1 plays an identical role both in hDPSCs and mDPCs in Runx2 exon 5 inclusion and odontogenic differentiation. Overexpression of hnRNP A1 significantly suppressed the inclusion of Runx2 exon 5 (Fig. 4A), and hnRNP A1 knockdown markedly promoted the inclusion of Runx2 exon 5 (Fig. 4E). We also found that overexpression of hnRNP A1 inhibited the expression of Alp and Ocn in the differentiation of mDPCs (Fig. 4C). In addition, the formation of mineralized nodules was reduced in hnRNP A1 overexpressed mDPCs compared with the control group (Fig. 4D). On the contrary, knockdown of hnRNP A1 led to increased expression of Alp and Ocn and increased mineralized nodules (Fig. 4G,H). These findings demonstrated that hnRNP A1 contributed to the skipping of RUNX2 exon 5 and repressed odontogenic differentiation of mDPCs.

4. Discussion

Alternative splicing was considered as a ubiquitous regulatory mechanism of gene expression that generates multiple mRNA species from a single gene [22]. Recent studies have shown that alternative splicing plays a role in MSC differentiation [23,24]. The hDPSC is a type of human dental-tissue-derived hMSC, that possesses considerable differentiation capacity [18,25]. A few studies have shown that alternative splicing plays an essential role in the differentiation of hDPSC. For instance, Octamer-binding transcriptional factor 4A (OCT4A), one isoform derived from OCT4 alternative splicing, enhanced the differentiation capability of hDPSC [26,27]. RUNX2 consists of nine exons, several studies have demonstrated that the inclusion of exon 5 is essential for the function of RUNX2 [9,28]. Multiple studies have indicated that RUNX2 is essential for odontogenesis [3,4]. However, few studies focused on the regulatory mechanism of alternative splicing on RUNX2 exon 5. Our previous study showed that YBX1 enhances the inclusion of RUNX2 exon 5 [10]. In the current study, we showed that hnRNP A1 had an opposite function to YBX1 in regulating the inclusion of RUNX2 exon 5. The hnRNP A1 protein belongs to the hnRNP A/B subfamily and is traditionally considered to be a splicing repressor [29]. The DNA sequence of human RUNX2 exon 5 is highly conserved in mouse, with only one nucleotide substitution and the amino acid sequences are identical. In this

study, through gain- and loss-of-function experiments, we found that hnRNP A1 suppressed the inclusion of exon 5 in both human and mouse cells, suggesting that the inhibitory effect of hnRNP A1 on RUNX2 exon 5 inclusion is conserved in both species. This finding is complementary to the alternative splicing mechanism of RUNX2 exon 5.

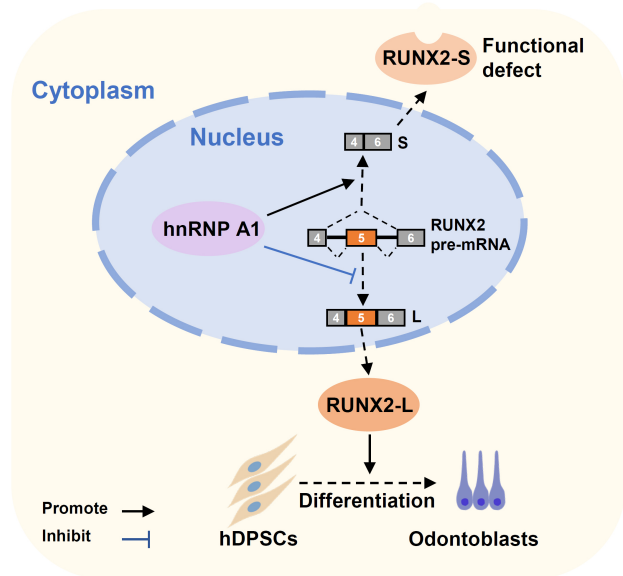


Fig. 5. A schematic model of hnRNP A1 inhibits RUNX2 exon 5 inclusion and hDPSCs differentiation. HnRNP A1 represses RUNX2 exon 5 inclusion, decreases the expression of full-length functional RUNX2 protein, and leads to the suppression of hDPSCs' odontogenic differentiation.

Several studies have shown that the function of hnRNP A1 in stem cell differentiation can be achieved by regulating alternative splicing or transcription [15,16]. Fang *et al.* [15] found that the ubiquitination of hnRNP A1 enhanced the exclusion of Arhgap1 exon 2, which ultimately impaired the differentiation of hematopoietic stem/progenitor cells. In another study, Huang *et al.* [16] found that hnRNP A1 promoted the differentiation of embryonic stem cells into smooth muscle cells (SMC) by directly binding to the promoter of SMC differentiation genes. However, the role of hnRNP A1 in differentiation of hDPSCs was poorly understood. Our current study showed that hnRNP A1 repressed the differentiation of hDPSCs by the reduction of the expression of ALP and OCN and the formation of mineralized nodules. These findings suggested that hnRNP A1 participated in the stem cell differentiation, and that the different roles of hnRNP A1 in differentiation of different stem cells may be related to the diversity of stem cell types.

5. Conclusions

In conclusion, we elucidated the roles of the RNA binding protein hnRNP A1 in the alternative splicing of RUNX2 exon 5 and the differentiation of hDPSCs and mDPCs. We discovered a novel inhibitory mechanism of RUNX2 exon 5 inclusion and the differentiation of dental mesenchymal cells (Fig. 5).

Availability of Data and Materials

Data supporting the findings of this study are available from the corresponding author upon reasonable request.

Author Contributions

JG and RJ designed the research study. YZ and JH performed the research. YZ, JH and LY conducted the statistical analysis of data. YZ, JG and RJ were responsible for writing of manuscript. YZ, JH, LY, RJ and JG contributed to the manuscript review and editing. All authors read and approved the final submitted manuscript.

Ethics Approval and Consent to Participate

This study was conducted in accordance with the Declaration of Helsinki. The collection of human dental pulp tissues was approved by the Ethics Committee of the School and Hospital of Stomatology at Wuhan University (2019-A47). Informed consent was obtained from every participant. The use of animal tissues was approved by the Animal Welfare and Ethics Committee of the School and Hospital of Stomatology at Wuhan University (S07922090F).

Acknowledgment

We would like to acknowledge the contribution to the dental pulp tissue collection of Xiulin Ran and Yujing Zhang, in the Department of Endodontics, School & Hospital of Stomatology, Wuhan University, Wuhan, 430079, China.

Funding

This study was supported by National Natural Science Foundation of China (Grant No. 81970933).

Conflict of Interest

The authors declare no conflict of interest.

Supplementary Material

Supplementary material associated with this article can be found, in the online version, at <https://doi.org/10.31083/j.fbl2807139>.

References

- [1] Komori T. Regulation of Proliferation, Differentiation and Functions of Osteoblasts by Runx2. *International Journal of Molecular Sciences*. 2019; 20: 1694.
- [2] James MJ, Järvinen E, Wang XP, Thesleff I. Different roles of Runx2 during early neural crest-derived bone and tooth development. *Journal of Bone and Mineral Research: the Official Journal of the American Society for Bone and Mineral Research*. 2006; 21: 1034–1044.
- [3] D'Souza RN, Aberg T, Gaikwad J, Cavender A, Owen M, Karsenty G, *et al*. Cbfa1 is required for epithelial-mesenchymal interactions regulating tooth development in mice. *Development*. 1999; 126: 2911–2920.
- [4] Aberg T, Wang XP, Kim JH, Yamashiro T, Bei M, Rice R, *et al*. Runx2 mediates FGF signaling from epithelium to mesenchyme during tooth morphogenesis. *Developmental Biology*. 2004; 270: 76–93.
- [5] Crute BE, Lewis AF, Wu Z, Bushweller JH, Speck NA. Biochemical and biophysical properties of the core-binding factor alpha2 (AML1) DNA-binding domain. *The Journal of Biological Chemistry*. 1996; 271: 26251–26260.
- [6] Kagoshima H, Shigesada K, Satake M, Ito Y, Miyoshi H, Ohki M, *et al*. The Runt domain identifies a new family of heteromeric transcriptional regulators. *Trends in Genetics: TIG*. 1993; 9: 338–341.
- [7] Vimalraj S, Arumugam B, Miranda PJ, Selvamurugan N. Runx2: Structure, function, and phosphorylation in osteoblast differentiation. *International Journal of Biological Macromolecules*. 2015; 78: 202–208.
- [8] Kim HJ, Kim WJ, Ryoo HM. Post-Translational Regulations of Transcriptional Activity of RUNX2. *Molecules and Cells*. 2020; 43: 160–167.
- [9] Makita N, Suzuki M, Asami S, Takahata R, Kohzaki D, Kobayashi S, *et al*. Two of four alternatively spliced isoforms of RUNX2 control osteocalcin gene expression in human osteoblast cells. *Gene*. 2008; 413: 8–17.
- [10] Shen J, She W, Zhang F, Guo J, Jia R. YBX1 Promotes the Inclusion of RUNX2 Alternative Exon 5 in Dental Pulp Stem Cells. *International Journal of Stem Cells*. 2022; 15: 301–310.
- [11] Bekenstein U, Soreq H. Heterogeneous nuclear ribonucleoprotein A1 in health and neurodegenerative disease: from structural insights to post-transcriptional regulatory roles. *Molecular and Cellular Neurosciences*. 2013; 56: 436–446.
- [12] Clarke JP, Thibault PA, Salapa HE, Levin MC. A Comprehensive Analysis of the Role of hnRNP A1 Function and Dysfunction in the Pathogenesis of Neurodegenerative Disease. *Frontiers in Molecular Biosciences*. 2021; 8: 659610.
- [13] Jean-Philippe J, Paz S, Caputi M. hnRNP A1: the Swiss army knife of gene expression. *International Journal of Molecular Sciences*. 2013; 14: 18999–19024.
- [14] Roy R, Huang Y, Seckl MJ, Pardo OE. Emerging roles of hnRNP A1 in modulating malignant transformation. *Wiley Interdisciplinary Reviews. RNA*. 2017; 8: 10.1002/wrna.1431.
- [15] Fang J, Bolanos LC, Choi K, Liu X, Christie S, Akunuru S, *et al*. Ubiquitination of hnRNP A1 by TRAF6 links chronic innate immune signaling with myelodysplasia. *Nature Immunology*. 2017; 18: 236–245.
- [16] Huang Y, Lin L, Yu X, Wen G, Pu X, Zhao H, *et al*. Functional involvements of heterogeneous nuclear ribonucleoprotein A1 in smooth muscle differentiation from stem cells *in vitro* and *in vivo*. *Stem Cells*. 2013; 31: 906–917.
- [17] Gronthos S, Brahimi J, Li W, Fisher LW, Cherman N, Boyde A, *et al*. Stem cell properties of human dental pulp stem cells. *Journal of Dental Research*. 2002; 81: 531–535.
- [18] Nuti N, Corallo C, Chan BMF, Ferrari M, Gerami-Naimi B. Multipotent Differentiation of Human Dental Pulp Stem Cells: a Literature Review. *Stem Cell Reviews and Reports*. 2016; 12: 511–523.
- [19] Goto N, Fujimoto K, Fujii S, Ida-Yonemochi H, Ohshima H, Kawamoto T, *et al*. Role of MSX1 in Osteogenic Differentia-

- tion of Human Dental Pulp Stem Cells. *Stem Cells International*. 2016; 2016: 8035759.
- [20] Gronthos S, Mankani M, Brahimi J, Robey PG, Shi S. Postnatal human dental pulp stem cells (DPSCs) *in vitro* and *in vivo*. *Proceedings of the National Academy of Sciences of the United States of America*. 2000; 97: 13625–13630.
- [21] Yu C, Guo J, Liu Y, Jia J, Jia R, Fan M. Oral squamous cancer cell exploits hnRNP A1 to regulate cell cycle and proliferation. *Journal of Cellular Physiology*. 2015; 230: 2252–2261.
- [22] Baralle FE, Giudice J. Alternative splicing as a regulator of development and tissue identity. *Nature Reviews. Molecular Cell Biology*. 2017; 18: 437–451.
- [23] Park JW, Fu S, Huang B, Xu RH. Alternative splicing in mesenchymal stem cell differentiation. *Stem Cells*. 2020; 38: 1229–1240.
- [24] Fiszbein A, Kornblihtt AR. Alternative splicing switches: Important players in cell differentiation. *BioEssays: News and Reviews in Molecular, Cellular and Developmental Biology*. 2017; 39: 10.1002/bies.201600157.
- [25] Sabbagh J, Ghassibe-Sabbagh M, Fayyad-Kazan M, Al-Nemer F, Fahed JC, Berberi A, *et al.* Differences in osteogenic and odontogenic differentiation potential of DPSCs and SHED. *Journal of Dentistry*. 2020; 101: 103413.
- [26] Ferro F, Spelat R, D'Aurizio F, Puppato E, Pandolfi M, Beltrami AP, *et al.* Dental pulp stem cells differentiation reveals new insights in Oct4A dynamics. *PloS one*. 2012; 7: e41774.
- [27] Liu L, Wu L, Wei X, Ling J. Induced overexpression of Oct4A in human dental pulp cells enhances pluripotency and multilineage differentiation capability. *Stem Cells and Development*. 2015; 24: 962–972.
- [28] Ge J, Guo S, Fu Y, Zhou P, Zhang P, Du Y, *et al.* Dental Follicle Cells Participate in Tooth Eruption via the RUNX2-MiR-31-SATB2 Loop. *Journal of Dental Research*. 2015; 94: 936–944.
- [29] Bruun GH, Doktor TK, Borch-Jensen J, Masuda A, Krainer AR, Ohno K, *et al.* Global identification of hnRNP A1 binding sites for SSO-based splicing modulation. *BMC Biology*. 2016; 14: 54.